Title
Convolution Lagrangian perturbation theory for biased tracers

Journal
Monthly Notices of the Royal Astronomical Society, 429(2)

ISSN
0035-8711

Authors
Carlson, Jordan
Reid, Beth
White, Martin

Publication Date
2013-02-21

DOI
10.1093/mnras/sts457

Peer reviewed

Mon. Not. R. Astron. Soc. **000**, 1–12 (0000) Printed 20 November 2012 (MN LaTeX style file v2.2)

Convolution Lagrangian Perturbation Theory for Biased Tracers

Jordan Carlson[1⋆], Beth Reid[2], and Martin White[1,2]
[1] *Department of Physics, University of California, Berkeley, CA 94720, USA*
[2] *Lawrence Berkeley National Laboratory, 1 Cyclotron Road, Berkeley, CA 94720, USA*

20 November 2012

ABSTRACT
We present a new formulation of Lagrangian perturbation theory which allows accurate predictions of the real- and redshift-space correlation functions of the mass field and dark matter halos. Our formulation involves a non-perturbative resummation of Lagrangian perturbation theory and indeed can be viewed as a partial resummation of the formalism of Matsubara (2008a,b) in which we keep exponentiated all of the terms which tend to a constant at large separation. One of the key features of our method is that we naturally recover the Zel'dovich approximation as the lowest order of our expansion for the matter correlation function. We compare our results against a suite of N-body simulations and obtain good agreement for the correlation functions in real-space and for the monopole correlation function in redshift space. The agreement becomes worse for higher multipole moments of the redshift-space, halo correlation function. Our formalism naturally includes non-linear bias and explains the strong bias-dependence of the multipole moments of the redshift-space correlation function seen in N-body simulations.

Key words: gravitation; galaxies: haloes; galaxies: statistics; cosmological parameters; large-scale structure of Universe

1 INTRODUCTION

The observed large-scale structure (LSS) of the universe is a pillar of modern observational cosmology, providing a window into the primordial fluctuations, expansion history, and growth rate of perturbations, as well as allowing tests of the theory of gravity on the largest accessible scales. The two-point correlation function (or its Fourier transform) is a useful and relatively simple compression of the cosmological information of interest. However, the interpretation of LSS statistics is hampered by two primary uncertainties: LSS tracers (e.g., galaxies, Ly-α forest, 21 cm) are *biased* relative to the underlying matter density field and are observed in redshift space. On very large scales these two effects are simple linear transformations of the underlying matter density field (Kaiser 1987; Efstathiou et al. 1988), while on Mpc scales, the dynamics are highly non-linear, and N-body simulations seem to be required for quantitative accuracy. However, on intermediate or quasi-linear scales there is hope that observable quantities for biased tracers may be accurately modeled semi-analytically by extending perturbation theory beyond linear order (see, Taruya, Nishimichi & Saito 2010; Reid & White 2011; Okamura, Taruya, & Matsubara 2011; Elia et al. 2011; Crocce, Scoccimarro, & Bernardeau 2012; Vlah et al. 2012, for recent work in this direction). Matsubara (2008a,b) introduced a new perturbative scheme (which we shall refer to as Lagrangian Resummation Theory; LRT) which addresses both non-linear biasing and redshift space distortions in a unified framework based on Lagrangian perturbation theory and that substantially improves upon standard perturbation theory for the description of both matter and dark matter halo clustering in the quasilinear regime (Padmanabhan & White 2009; Noh, White & Padmanabhan 2009; Reid & White 2011; Sato & Matsubara 2011; Rampf 2012). In this paper propose a new resummation scheme which extends the work of Matsubara (2008a,b) and results in a more accurate expression for the two-point correlation function in both real- and redshift-space for both matter and dark matter halos.

There are several advantages to adopting a Lagrangian description of the LSS. The well-known Zel'dovich approximation (Zel'dovich 1970) provides a one time-step, reasonably accurate approximation to the non-linear density field by displacing Lagrangian particles by the linear theory displacement field (for a recent examination, see Tassev & Zaldarriaga 2012a,b). A distinctive feature of the present work is that we recover the Zel'dovich result exactly as a limit of our expression for the correlation function of matter (which is not the case in a similar study by McCullagh & Szalay 2012). The clustering of dark matter halos is of greater interest for the interpretation of galaxy redshift surveys, since modern galaxy formation models assume that galaxies form and reside in the gravitational potential wells of dark matter halos. Again, the LRT approach is advantageous since a local Lagrangian biasing scheme provides a better description of the biasing of dark matter halos in N-body simulations compared with local Eulerian bias (Roth & Porciani 2011; Baldauf et al. 2012;

⋆ Email: jwgcarlson@berkeley.edu

Chan, Scoccimarro, & Sheth 2012) and can be extended to include a continuous galaxy formation history (Wang & Szalay 2012).

The outline of the paper is as follows. We begin with a brief review of Lagrangian perturbation theory in Section 2. In Section 3, we present our results within the context of the Zel'dovich approximation, in which many of the main physical effects are present but the algebra is simplified. In Section 4, we extend our results to the next higher order in perturbation theory, with most of the details and formulae being relegated to Appendices. In Section 5 we present a detailed comparison of our analytic theory with high-precision N-body simulations. We conclude in Section 6.

For plots and numerical comparisons we assume a ΛCDM cosmology with $\Omega_m = 0.274$, $\Omega_\Lambda = 0.726$, $h = 0.7$, $n = 0.95$, and $\sigma_8 = 0.8$. Our simulation data are derived from a suite of 20 N-body simulations run with the TreePM code described in White (2002). Each simulation employed 1500^3 equal mass ($m_p \simeq 7.6 \times 10^{10}\, h^{-1} M_\odot$) particles in a periodic cube of side length $1.5\, h^{-1}$Gpc as described in (Reid & White 2011; White et al. 2011).

2 BACKGROUND AND REVIEW

In this section we provide a brief review of cosmological perturbation theory, focusing on the Lagrangian formulation[1] (Buchert 1989; Moutarde et al. 1991; Hivon et al. 1995; Taylor & Hamilton 1996). This material should be sufficient to remind the reader of some essential terminology, and to establish our notational conventions. Our discussion is largely drawn from Matsubara (2008a,b) to which we refer the reader for further details.

2.1 Basic definitions

Cosmological perturbation theory concerns itself with predicting the clustering properties of cosmological fluids. In the context of large-scale structure, (i.e., at late times when baryons and photons have completely decoupled), the only relevant fluid is the matter fluid, which, on all but the very smallest scales, interacts only through self-gravitational coupling.

The matter fluid is idealized as a single-streaming, pressureless dust, characterized at any time t by its mass density $\rho(\boldsymbol{x}, t)$ and peculiar velocity field $\boldsymbol{v}(\boldsymbol{x}, t)$. Following common convention, we let $\boldsymbol{x}$ denote position in comoving coordinates, and t denote proper time for a comoving observer. The mean value $\bar{\rho}(t) = \langle \rho(\boldsymbol{x}, t) \rangle$ of the mass density decreases as the universe expands like $\bar{\rho} \propto a^{-3}$, where $a(t)$ is the cosmic scale factor. (Here and hereafter, we drop the explicit time dependence in equations where all quantities are to be evaluated at the same time.) Deviations from homogeneity are expressed in terms of the density contrast $\delta(\boldsymbol{x}, t)$, defined by the relation $\rho(\boldsymbol{x}) = \bar{\rho}[1 + \delta(\boldsymbol{x})]$.

The most important statistical quantities that can be formed from these fields are the 2-point correlation function,

$$\xi(\boldsymbol{r}) = \langle \delta(\boldsymbol{x}) \delta(\boldsymbol{x} + \boldsymbol{r}) \rangle, \tag{1}$$

and its Fourier transform, the power spectrum $P(\boldsymbol{k})$, defined by

$$\langle \tilde{\delta}(\boldsymbol{k}) \tilde{\delta}(\boldsymbol{k}') \rangle = (2\pi)^3 \delta_D(\boldsymbol{k} + \boldsymbol{k}') P(\boldsymbol{k}). \tag{2}$$

Here δ_D denotes the 3-dimensional Dirac delta function, and we use the Fourier transform convention

$$F(\boldsymbol{x}) = \int \frac{d^3k}{(2\pi)^3}\, \tilde{F}(\boldsymbol{k}) e^{i\boldsymbol{k}\cdot\boldsymbol{x}}. \tag{3}$$

Angle brackets around a cosmological field, e.g. $\langle F \rangle$, signify an ensemble average of that quantity over all possible realizations of our universe; in most cases of interest, ergodicity allows us to replace these ensemble averages with spatial averages over a sufficiently large cosmic volume.

2.2 Lagrangian perturbation theory

In the Lagrangian approach to cosmological fluid dynamics, one traces the trajectory of an individual fluid element through space and time. For a fluid element located at position $\boldsymbol{q}$ at some initial time t_0, its position at subsequent times can be written in terms of the Lagrangian displacement field $\boldsymbol{\Psi}$,

$$\boldsymbol{x}(\boldsymbol{q}, t) = \boldsymbol{q} + \boldsymbol{\Psi}(\boldsymbol{q}, t), \tag{4}$$

where $\boldsymbol{\Psi}(\boldsymbol{q}, t_0) = 0$. Every element of the fluid is uniquely labeled by its Lagrangian coordinate $\boldsymbol{q}$, so that for a fixed t we may view the mapping $\boldsymbol{q} \leftrightarrow \boldsymbol{x}$ as a simple change of variable.

The displacement field $\boldsymbol{\Psi}(\boldsymbol{q}, t)$ fully specifies the motion of the cosmological fluid. The aim of Lagrangian Perturbation Theory (LPT) is to find a perturbative solution for the displacement field,

$$\boldsymbol{\Psi}(\boldsymbol{q}, t) = \boldsymbol{\Psi}^{(1)}(\boldsymbol{q}, t) + \boldsymbol{\Psi}^{(2)}(\boldsymbol{q}, t) + \boldsymbol{\Psi}^{(3)}(\boldsymbol{q}, t) + \cdots. \tag{5}$$

The first order solution is the well-known Zel'dovich approximation (Zel'dovich 1970). Explicit solutions are known up to fourth order (Rampf & Buchert 2012).

The continuity equation

$$[1 + \delta(\boldsymbol{x}, t)] d^3x = [1 + \delta_0(\boldsymbol{q})] d^3q \tag{6}$$

expresses the fact that, for a smoothly evolving fluid, an element d^3q centered at $\boldsymbol{q}$ at time t_0 is transformed into an element d^3x centered at $\boldsymbol{x}(\boldsymbol{q}, t)$ at time t. The initial time t_0 may be taken to be early enough that the initial matter fluctuations $\delta_0(\boldsymbol{q})$ are arbitrarily small, so that we may formally express the Eulerian density field in terms of the Lagrangian displacement field as

$$1 + \delta(\boldsymbol{x}, t) = \int d^3q\, \delta_D[\boldsymbol{x} - \boldsymbol{q} - \boldsymbol{\Psi}(\boldsymbol{q}, t)]. \tag{7}$$

2.3 Biased tracers

Although small, the initial density fluctuations $\delta_0(\boldsymbol{q})$ provide the seeds for subsequent structure formation. In this paper we restrict ourselves to a local Lagrangian bias model, which posits that the locations of discrete tracers at some late time t are determined by the overdensities in the initial matter density field. More explicitly, let $\delta_R(\boldsymbol{q})$ denote the matter density contrast at the initial time t_0, smoothed on some scale R. (In the end the value of this smoothing scale will turn out to be irrelevant, but its use helps ensure that intermediate quantities are well-behaved.) Consider a collection of discrete tracers X, where X might denote galaxies of a particular type, or halos of a particular mass range, etc. The locations $\{\boldsymbol{x}_i\}$ of these tracers at time t may be identified with particular points $\{\boldsymbol{q}_i\}$ in the initial density field by inverting Eqn. 4. Our hypothesis is that these initial locations $\{\boldsymbol{q}_i\}$ are drawn from a distribution that is a locally biased function of the smoothed matter density field, i.e.

$$\rho_X(\boldsymbol{q}) = \bar{\rho}_X F[\delta_R(\boldsymbol{q})]. \tag{8}$$

[1] See Bernardeau et al. (2002) for a comprehensive (though somewhat dated) review of Eulerian perturbation theory.

Here $\bar{\rho}_X$ is the mean comoving number density of our tracer X and the function $F(\delta)$ is called the Lagrangian bias function. The perturbations in $\rho_X(\boldsymbol{q})$ are $O(\delta_R(\boldsymbol{q}))$ and therefore also arbitrarily small. When this biasing relation is viewed in Eulerian coordinates, it is non-local: $\rho_X(\boldsymbol{x})$ is depends on the matter density at points other than $\boldsymbol{x}$ (e.g., Catelan et al. 1998; Matsubara 2011). The corresponding non-local Eulerian bias terms can be most easily seen in their contribution to the bispectrum of halos (Baldauf et al. 2012; Chan, Scoccimarro, & Sheth 2012). Matsubara (2011) extends the formalism from Matsubara (2008a,b) that we have adopted here to include non-local Lagrangian bias as well, e.g., the peaks bias model (Bardeen et al. 1986), but we do not explore those extensions here.

2.4 Redshift space

While analyzing the clustering of biased tracers is difficult enough, for modern surveys we must also deal with the complication of redshift space distortions. The position of an object, located at true comoving position $\boldsymbol{x}$, will be mis-identified due to its peculiar velocity along the line-of-sight, as

$$\boldsymbol{s} = \boldsymbol{x} + \frac{\hat{z}\cdot\boldsymbol{v}(\boldsymbol{x})}{aH}\hat{z}. \tag{9}$$

In this work we adopt the standard "plane-parallel" or "distant-observer" approximation, in which the line-of-sight direction to each object is taken to be the fixed direction $\hat{z}$. While this may seem a poor assumption for modern wide-area surveys, it has been shown to be sufficient within the level of current error bars (e.g., Figure 10 of Samushia, Percival, & Raccanelli 2012).

In the Lagrangian approach, including redshift-space distortions requires only a simple additive offset of the displacement field. The peculiar velocity of a fluid element, labeled by its Lagrangian coordinate $\boldsymbol{q}$, is at any time given by

$$\boldsymbol{v}(\boldsymbol{q}) = a\dot{\boldsymbol{x}}(\boldsymbol{q}) = a\dot{\boldsymbol{\Psi}}(\boldsymbol{q}). \tag{10}$$

So in redshift space, the apparent displacement of the fluid element is

$$\boldsymbol{\Psi}^s = \boldsymbol{\Psi} + \frac{\hat{z}\cdot\dot{\boldsymbol{\Psi}}}{H}\hat{z}. \tag{11}$$

To a good approximation the time dependence of the nth order term in Eq. (5) is given by $\boldsymbol{\Psi}^{(n)} \propto D^n$. Therefore $\dot{\boldsymbol{\Psi}}^{(n)} = nHf\boldsymbol{\Psi}^{(n)}$, where $f = d\log D/d\log a$ is the growth rate, often approximated as $f \approx \Omega_m^{0.6}$. The mapping to redshift space may then be achieved, order-by-order, via the matrix

$$R_{ij}^{(n)} = \delta_{ij} + nf\hat{z}_i\hat{z}_j, \tag{12}$$

as $\boldsymbol{\Psi}^{s(n)} = R^{(n)}\boldsymbol{\Psi}^{(n)}$.

3 ZEL'DOVICH APPROXIMATION

In this section we present a derivation of our new result in the simplified setting of the Zel'dovich approximation (see also Bond & Couchman 1988). This allows us to sketch the main idea of our approach while avoiding many of the complications inherent in perturbative calculations. Several key points regarding the form of the solution are made along the way.

Our starting point is the continuity equation

$$[1+\delta_X(\boldsymbol{x},t)]\,d^3x = [1+\delta_X(\boldsymbol{q},t_0)]\,d^3q, \tag{13}$$

expressing the conservation of number density for the tracer X between times t_0 and t. Invoking the hypothesis of local Lagrangian biasing, the quantity on the right-hand side is

$$1+\delta_X(\boldsymbol{q},t_0) = F[\delta_R(\boldsymbol{q})], \tag{14}$$

so that

$$1+\delta_X(\boldsymbol{x},t) = \left|\frac{\partial\boldsymbol{x}}{\partial\boldsymbol{q}}\right|^{-1} F[\delta_R(\boldsymbol{q})] \tag{15}$$

$$= \int d^3q\, F[\delta_R(\boldsymbol{q})]\delta_D\left[\boldsymbol{x}-\boldsymbol{q}-\boldsymbol{\Psi}(\boldsymbol{q},t)\right]. \tag{16}$$

In the following, we will suppress the explicit dependence on t when there is no risk of ambiguity. We now replace the delta function with its Fourier representation, and also introduce the Fourier transform $\tilde{F}(\lambda)$ of $F(\delta)$,

$$1+\delta_X(\boldsymbol{x}) = \int d^3q\, F[\delta_R(\boldsymbol{q})]\int\frac{d^3k}{(2\pi)^3}\,e^{i\boldsymbol{k}\cdot[\boldsymbol{x}-\boldsymbol{q}-\boldsymbol{\Psi}(\boldsymbol{q})]} \tag{17}$$

$$= \int d^3q\int\frac{d^3k}{(2\pi)^3}\int\frac{d\lambda}{2\pi}\,\tilde{F}(\lambda)\,e^{i\{\lambda\delta_R(\boldsymbol{q})+\boldsymbol{k}\cdot[\boldsymbol{x}-\boldsymbol{q}-\boldsymbol{\Psi}(\boldsymbol{q})]\}}. \tag{18}$$

The 2-point correlation function $\xi_X(\boldsymbol{r}) = \langle\delta_X(\boldsymbol{x}_1)\delta_X(\boldsymbol{x}_2)\rangle$ for the biased tracer X is then given by

$$1+\xi_X(\boldsymbol{r}) = \int d^3q_1\,d^3q_2\int\frac{d^3k_1}{(2\pi)^3}\frac{d^3k_2}{(2\pi)^3}\,e^{i\boldsymbol{k}_1\cdot(\boldsymbol{x}_1-\boldsymbol{q}_1)}e^{i\boldsymbol{k}_2\cdot(\boldsymbol{x}_2-\boldsymbol{q}_2)} \times \int\frac{d\lambda_1}{2\pi}\frac{d\lambda_2}{2\pi}\,\tilde{F}(\lambda_1)\tilde{F}(\lambda_2)\left\langle e^{i[\lambda_1\delta_1+\lambda_2\delta_2-\boldsymbol{k}_1\cdot\boldsymbol{\Psi}_1-\boldsymbol{k}_2\cdot\boldsymbol{\Psi}_2]}\right\rangle \tag{19}$$

where $\delta_a \equiv \delta_R(\boldsymbol{q}_a)$, $\boldsymbol{\Psi}_a \equiv \boldsymbol{\Psi}(\boldsymbol{q}_a)$, and $\boldsymbol{r} = \boldsymbol{x}_2 - \boldsymbol{x}_1$. By statistical homogeneity, the expectation value above depends only on the difference in Lagrangian coordinates, $\boldsymbol{q} = \boldsymbol{q}_2 - \boldsymbol{q}_1$. The change of variables $\{\boldsymbol{q}_1,\boldsymbol{q}_2\}\to\{\boldsymbol{q},\boldsymbol{Q}=(\boldsymbol{q}_1+\boldsymbol{q}_2)/2\}$ then leads to

$$1+\xi_X(\boldsymbol{r}) = \int d^3q\int\frac{d^3k}{(2\pi)^3}e^{i\boldsymbol{k}\cdot(\boldsymbol{q}-\boldsymbol{r})}\int\frac{d\lambda_1}{2\pi}\frac{d\lambda_2}{2\pi}\,\tilde{F}_1\tilde{F}_2\,K(\boldsymbol{q},\boldsymbol{k},\lambda_1,\lambda_2), \tag{20}$$

where we have defined

$$K(\boldsymbol{q},\boldsymbol{k},\lambda_1,\lambda_2) = \left\langle e^{i(\lambda_1\delta_1+\lambda_2\delta_2+\boldsymbol{k}\cdot\boldsymbol{\Delta})}\right\rangle, \tag{21}$$

and $\Delta \equiv \boldsymbol{\Psi}_2 - \boldsymbol{\Psi}_1$. This expression is the exact configuration space analog of Eq. (9) in Matsubara (2008b).

The cumulant expansion theorem allows us to expand the expectation value in Eq. (21) in terms of cumulants,

$$\langle e^{iX}\rangle = \exp\left[\sum_{N=1}^{\infty}\frac{i^N}{N!}\langle X^N\rangle_c\right], \tag{22}$$

where $\langle X^N\rangle_c$ denotes the Nth cumulant of the random variable X. The field $\delta_R(\boldsymbol{q})$ is a smoothed version of the linear density field $\delta_L(\boldsymbol{q})$, and is therefore Gaussian. Within the Zel'dovich approximation, the displacement field

$$\boldsymbol{\Psi}(\boldsymbol{q}) = \int\frac{d^3k}{(2\pi)^3}\,e^{i\boldsymbol{k}\cdot\boldsymbol{q}}\frac{i\boldsymbol{k}}{k^2}\tilde{\delta}_L(\boldsymbol{k}), \tag{23}$$

is linear in δ_L, hence also Gaussian. Thus, in the applying the cumulant expansion theorem to Eq. (21), only the second cumulant survives,

$$\left\langle(\lambda_1\delta_1+\lambda_2\delta_2+\boldsymbol{k}\cdot\boldsymbol{\Delta})^2\right\rangle_c = (\lambda_1^2+\lambda_2^2)\sigma_R^2 + A_{ij}k_ik_j + 2\lambda_1\lambda_2\xi_R + 2(\lambda_1+\lambda_2)U_ik_i, \tag{24}$$

where we have defined

$$\sigma_R^2 = \langle\delta_1^2\rangle_c = \langle\delta_2^2\rangle_c, \qquad \xi_R(\boldsymbol{q}) = \langle\delta_1\delta_2\rangle_c, \tag{25}$$

$$A_{ij}(\boldsymbol{q}) = \langle\Delta_i\Delta_j\rangle_c, \qquad U_i(\boldsymbol{q}) = \langle\delta_1\Delta_i\rangle_c = \langle\delta_2\Delta_i\rangle_c. \tag{26}$$

Eq. (21) then evaluates to

$$K = \exp\left[-\frac{1}{2}(\lambda_1^2+\lambda_2^2)\sigma_R^2 - \frac{1}{2}A_{ij}k_ik_j - \lambda_1\lambda_2\xi_R - (\lambda_1+\lambda_2)U_ik_i\right]. \tag{27}$$

The quantity σ_R^2 is simply the variance of the smoothed linear density field, while $\xi_R(\boldsymbol{q}) = \langle\delta_R(\boldsymbol{q}_1)\delta_R(\boldsymbol{q}_2)\rangle$ is the corresponding smoothed linear correlation function. The matrix A_{ij} may be decomposed as

$$A_{ij}(\boldsymbol{q}) = 2\left[\sigma_\eta^2 - \eta_\perp(q)\right]\delta_{ij} + 2\left[\eta_\perp(q) - \eta_\parallel(q)\right]\hat{q}_i\hat{q}_j, \tag{28}$$

where $\sigma_\eta^2 \equiv \frac{1}{3}\langle|\boldsymbol{\Psi}|^2\rangle$ is the 1-D dispersion of the displacement field, and $\eta_\parallel$ and $\eta_\perp$ are the transverse and longitudinal components of the Lagrangian 2-point function, $\eta_{ij}(\boldsymbol{q}) = \left\langle\Psi_i(\boldsymbol{q}_1)\Psi_j(\boldsymbol{q}_2)\right\rangle$. The vector $U_i(\boldsymbol{q}) = U(q)\,\hat{q}_i$ is the cross-correlation between the linear density field and the Lagrangian displacement field. In the Zel'dovich approximation these quantities are given by

$$\sigma_\eta^2 = \frac{1}{6\pi^2}\int_0^\infty dk\, P_L(k), \tag{29}$$

$$\eta_\perp(q) = \frac{1}{2\pi^2}\int_0^\infty dk\, P_L(k)\,\frac{j_1(kq)}{kq}, \tag{30}$$

$$\eta_\parallel(q) = \frac{1}{2\pi^2}\int_0^\infty dk\, P_L(k)\left[j_0(kq) - 2\frac{j_1(kq)}{kq}\right], \tag{31}$$

$$U(q) = -\frac{1}{2\pi^2}\int_0^\infty dk\, kP_L(k)\, j_1(kq). \tag{32}$$

Up to factors of 2 and f, these expressions are identical to the Eulerian velocity correlators in linear theory (e.g. Fisher 1995; Reid & White 2011), which is not surprising since $\boldsymbol{v}_L = f\Psi$ in the Zel'dovich approximation.

3.1 Exact results for matter

At this point we pause to consider the unbiased case, where $F(\delta) = 1$ or $\tilde{F}(\lambda) = 2\pi\delta_D(\lambda)$. In this limit Eq. (20) reduces to

$$1 + \xi^{(ZA)}(\boldsymbol{r}) = \int d^3q \int \frac{d^3k}{(2\pi)^3} e^{i\boldsymbol{k}\cdot(\boldsymbol{q}-\boldsymbol{r})} e^{-\frac{1}{2}A_{ij}k_ik_j} \tag{33}$$

$$= \int \frac{d^3q}{(2\pi)^{3/2}|A|^{1/2}} e^{-\frac{1}{2}(\boldsymbol{r}-\boldsymbol{q})^\top \mathbf{A}^{-1}(\boldsymbol{r}-\boldsymbol{q})}, \tag{34}$$

after carrying out the Gaussian integral over $\boldsymbol{k}$ analytically. This is an exact expression for the real-space matter correlation function within the Zel'dovich approximation. It has the apparent form of a Gaussian convolution kernel, except for the fact that the matrix A_{ij} is a function of $\boldsymbol{q}$. Indeed, we see that $\xi^{(ZA)}$ arises entirely from the scale-dependence of this Lagrangian correlator.

The smoothing of the acoustic feature is often modeled as a convolution of the linear correlation function by a Gaussian kernel, with the smoothing scale estimated at lowest order by $2\sigma_\eta^2$. We can massage our expression into a similar form by noting that A_{ij} can be written as the sum

$$A_{ij}(\boldsymbol{q}) = B_{ij} + C_{ij}(\boldsymbol{q}), \tag{35}$$

where $B_{ij} = 2\sigma_\eta^2\delta_{ij}$ is scale-independent. Then, by the same reasoning as is used to show that the convolution of two Gaussians is a Gaussian, we can write

$$1 + \xi^{(ZA)}(\boldsymbol{r}) = \int \frac{d^3q}{(2\pi)^{3/2}|B|^{1/2}}\, e^{-\frac{1}{2}(\boldsymbol{r}-\boldsymbol{q})^\top \mathbf{B}^{-1}(\boldsymbol{r}-\boldsymbol{q})}[1+\chi(\boldsymbol{q})], \tag{36}$$

where we have defined

$$1 + \chi(\boldsymbol{q}) = \int \frac{d^3p}{(2\pi)^{3/2}|C|^{1/2}}\, e^{-\frac{1}{2}(\boldsymbol{q}-\boldsymbol{p})^\top \mathbf{C}^{-1}(\boldsymbol{q}-\boldsymbol{p})}. \tag{37}$$

Eq. (36) is a proper Gaussian convolution, since the matrix $\mathbf{B}$ is independent of $\boldsymbol{q}$. The quantity $\chi(\boldsymbol{q})$ may therefore be viewed as an analog of the linear correlation function. Indeed, the two are quite similar. These observations provide analytic justification to conventional wisdom, first pointed out in Bharadwaj (1996), that nonlinear structure growth causes a Gaussian smearing of the clustering signal. In our approach, this result is obtained at leading order, within the Zel'dovich approximation.

3.2 Perturbative expansion for biased tracers

Returning to the case of biased tracers, consider again Eq. (27). In the unbiased case the $\boldsymbol{k}$ integration in Eq. (20) took the form of a Gaussian integral, which we carried out analytically. In the biased case, we can achieve the same thing if we first partially expand Eq. (27) as

$$\begin{aligned} K \;=\;& e^{-\frac{1}{2}(\lambda_1^2+\lambda_2^2)\sigma_R^2} e^{-\frac{1}{2}\boldsymbol{k}^T A \boldsymbol{k}}\left[1 - \lambda_1\lambda_2\xi_R - (\lambda_1+\lambda_2)U_ik_i\right.\\ &+ \frac{1}{2}\lambda_1^2\lambda_2^2\xi_R^2 + \frac{1}{2}(\lambda_1+\lambda_2)^2U_iU_jk_ik_j\\ &+ \left.\lambda_1\lambda_2(\lambda_1+\lambda_2)\xi_RU_ik_i + O(P_L^3)\right]. \end{aligned} \tag{38}$$

We may justify this choice of expansion by noting that both $\xi_R(\boldsymbol{q})$ and $U_i(\boldsymbol{q})$ vanish in the large-scale limit $|\boldsymbol{q}| \to \infty$, while σ_R^2 and $A_{ij}(\boldsymbol{q})$ approach non-zero values. In the language of perturbation theory, keeping these terms exponentiated therefore amounts to an non-perturbative resummation of the dominant large-scale contributions.

Tassev & Zaldarriaga (2012a,b) have recently emphasized the importance of not splitting the effects of bulk flows across orders in perturbation theory. The resummation described above has this property, which is not shared by the resummations used in LRT or RPT (Crocce & Scoccimarro 2006).

To get from Eq. (38) to an expression for $\xi_X(\boldsymbol{r})$, we must integrate K over λ_1, λ_2, $\boldsymbol{k}$, and $\boldsymbol{q}$. The λ_1 and λ_2 integrations may be evaluated via the identity (Matsubara 2008b)

$$\int \frac{d\lambda}{2\pi}\,\tilde{F}(\lambda)\,(i\lambda)^n\, e^{-\frac{1}{2}\lambda^2\sigma_R^2} = \int \frac{d\delta}{\sqrt{2\pi}\sigma_R}\, e^{-\delta^2/2\sigma_R^2}\frac{d^nF}{d\delta^n} \equiv \left\langle F^{(n)}\right\rangle, \tag{39}$$

where $\left\langle F^{(n)}\right\rangle$ is the expectation value of the nth derivative of the Lagrangian bias function $F(\delta)$ (see Appendix A for details). Application of this identity leads to

$$L(\boldsymbol{q},\boldsymbol{k}) \;\equiv\; \int \frac{d\lambda_1}{2\pi}\frac{d\lambda_2}{2\pi}\,\tilde{F}(\lambda_1)\tilde{F}(\lambda_2)\,K(\boldsymbol{q},\boldsymbol{k},\lambda_1,\lambda_2) \tag{40}$$

$$\begin{aligned} =\;& e^{-\frac{1}{2}A_{ij}k_ik_j}\left[1 + \langle F'\rangle^2\xi_R + 2i\langle F'\rangle U_ik_i + \frac{1}{2}\langle F''\rangle^2\xi_R^2\right.\\ &- (\langle F''\rangle + \langle F'\rangle^2)U_iU_jk_ik_j + 2i\langle F'\rangle\langle F''\rangle\xi_RU_ik_i\\ &+ \left.O(P_L^3)\right]. \end{aligned} \tag{41}$$

The $\boldsymbol{k}$ integration reduces to a series of multi-variate Gaussian integrals of the form

$$\int \frac{d^3k}{(2\pi)^3}\, e^{-\frac{1}{2}A_{ij}k_ik_j}\, e^{i\boldsymbol{k}\cdot(\boldsymbol{q}-\boldsymbol{r})}\, k_{i_1}\cdots k_{i_r} \quad . \tag{42}$$

Appendix C reviews the relevant formulae. In the end we obtain

$$\begin{aligned} M(\boldsymbol{r},\boldsymbol{q}) &\equiv \int \frac{d^3k}{(2\pi)^3}\, e^{i\boldsymbol{k}\cdot(\boldsymbol{q}-\boldsymbol{r})} L(\boldsymbol{q},\boldsymbol{k}) \qquad (43)\\ &= \frac{1}{(2\pi)^{3/2}|A|^{1/2}}\, e^{-\frac{1}{2}(\boldsymbol{r}-\boldsymbol{q})^T\mathbf{A}^{-1}(\boldsymbol{r}-\boldsymbol{q})} \Big[1+\langle F'\rangle^2 \xi_R \\ &- 2\langle F'\rangle U_i g_i + \frac{1}{2}\langle F''\rangle^2 \xi_R^2 - (\langle F''\rangle + \langle F'\rangle^2) U_i U_j G_{ij} \\ &- 2\langle F'\rangle\langle F''\rangle \xi_R U_i g_i + O(P_L^3)\Big], \qquad (44) \end{aligned}$$

where

$$\boldsymbol{g} \equiv A^{-1}(\boldsymbol{q}-\boldsymbol{r}), \quad G_{ij} \equiv (A^{-1})_{ij} - g_i g_j. \qquad (45)$$

Our final expression for the correlation function is

$$1+\xi_X(\boldsymbol{r}) = \int d^3q\, M(\boldsymbol{r},\boldsymbol{q}). \qquad (46)$$

The remaining integration over $\boldsymbol{q}$ must be performed numerically.

Note well that, although our calculation is very similar to that of Matsubara (2008b), our result for $\xi_X(r)$ is *not* simply the Fourier transform of his Eq. (34) for $P_{\rm obj}(k)$ The difference lies in our choice of expansion in Eq. (38). As discussed previously, the matrix $A_{ij}(\boldsymbol{q})$ is the sum of a constant term $2\sigma_\eta^2\delta_{ij}$ and a scale-dependent remainder $C_{ij}(\boldsymbol{q})$. In Matsubara (2008b) only the constant piece is exponentiated while the rest is expanded, i.e.

$$K_{\rm Mat} = e^{-\frac{1}{2}(\lambda_1^2+\lambda_2^2)\sigma_R^2} e^{-\sigma_\eta^2 k^2} \left[1 - \frac{1}{2}\boldsymbol{k}^\top \mathbf{C}\boldsymbol{k} - \lambda_1\lambda_2\xi_R - (\lambda_1+\lambda_2)U_i k_i + \cdots\right]. \qquad (47)$$

Our approach may be seen as a partial resummation of the result of Matsubara (2008b), and as such we expect it to be more accurate on small scales.

Before we leave this section it is worth noting the manner in which the bias terms enter in Eq. (41). In particular note the term which goes as $\langle F'\rangle\langle F''\rangle$ at the end of the 3rd line and the $\langle F''\rangle^2$ term at the end of the 2nd line. For highly biased halos, assuming the peak-background split to compute the bias, $\langle F''\rangle \propto \langle F'\rangle^2 \propto b^2$, so these terms can come in with (apparently) large powers of b, beyond the b^2 terms which one would naturally expect in a 2-point function (see also Reid & White 2011). In our calculation using the Zel'dovich approximation and local Lagrangian bias we see these important contributions arise from 2nd order bias.

3.3 Redshift space

Thus far we have concentrated on real space results, however the transition to redshift space is easily achieved. Recall that the displacement field in redshift space is given by $\boldsymbol{\Psi}^s = \boldsymbol{\Psi} + H^{-1}(\hat{z}\cdot\dot{\boldsymbol{\Psi}})\hat{z}$. In the Zel'dovich approximation $\boldsymbol{\Psi} \propto D(t)$, so

$$\Psi_i^{s(ZA)} = \left(\delta_{ij} + f\hat{z}_i\hat{z}_j\right)\Psi_j^{(ZA)}. \qquad (48)$$

Our previous derivation remains valid, we need only make the substitutions

$$U_i \to U_i^s = (\delta_{ij} + f\hat{z}_i\hat{z}_j)U_j, \qquad (49)$$
$$A_{ij} \to A_{ij}^s = (\delta_{ik} + f\hat{z}_i\hat{z}_k)(\delta_{jl} + f\hat{z}_j\hat{z}_l)A_{kl}. \qquad (50)$$

This slightly complicates the evaluation of the $\boldsymbol{q}$ integration in Eq. (46), in that we can no longer use azimuthal symmetry to reduce it to a 2-D integral. Nevertheless, the full 3-D integral is still feasible numerically, and the redshift space correlation function $\xi_X^s(\boldsymbol{s})$ may be easily calculated.

3.4 Linear theory limit

Standard Eulerian perturbation theory describes an expansion for the power spectrum of the form,

$$P(k) = P^{(1)}(k) + P^{(2)}(k) + \cdots \qquad (51)$$

where $P^{(n)}$ is $O(P_L^n)$. Unfortunately this expansion does not translate into a well-defined perturbative expansion for $\xi(r)$, as the Fourier transform of $P^{(n)}$ diverges for $n > 1$. Nevertheless, the linear theory correlation function is well-defined, and our approach should reproduce this limit when P_L is small. We now show that this is indeed the case.

In the Zel'dovich approximation, the correlators A_{ij} and U_i are given by linear integrals of P_L,

$$\begin{aligned} A_{ij}(\boldsymbol{q}) &= \int \frac{d^3k}{(2\pi)^3}\left[2 - e^{i\boldsymbol{k}\cdot\boldsymbol{q}} - e^{-i\boldsymbol{k}\cdot\boldsymbol{q}}\right]\frac{-k_ik_j}{k^4}P_L(k), \\ U_i(\boldsymbol{q}) &= \int \frac{d^3k}{(2\pi)^3}\, e^{i\boldsymbol{k}\cdot\boldsymbol{q}}\, \frac{ik_i}{k^2}P_L(k). \end{aligned} \qquad (52)$$

The quantity $M(\boldsymbol{r},\boldsymbol{q})$ defined in Eq. (44) is therefore ill-defined in the limit $P_L \to 0$. To make our discussion precise, we replace the matrix A_{ij} in this expression by

$$B_{ij}(\boldsymbol{q}) = \beta^2\delta_{ij} + \epsilon A_{ij}(\boldsymbol{q}), \qquad (53)$$

where β is a regularizing parameter that will eventually be set to zero, and ϵ is a book-keeping parameter to help keep track of powers of P_L. Thus we write

$$\begin{aligned} 1+\xi_X(\boldsymbol{r}) &= \lim_{\beta\to 0}\int \frac{d^3q}{(2\pi)^{3/2}|B|^{1/2}}\, e^{-\frac{1}{2}(\boldsymbol{r}-\boldsymbol{q})^\top\mathbf{B}^{-1}(\boldsymbol{r}-\boldsymbol{q})}\,[1+ \\ &\quad 2\epsilon\langle F'\rangle \boldsymbol{U}^\top\mathbf{B}^{-1}(\boldsymbol{r}-\boldsymbol{q}) + \epsilon\langle F'\rangle^2\xi_L + O(\epsilon^2)] \qquad (54)\\ &= 1 + \epsilon\xi_X^{(1)}(\boldsymbol{r}) + \epsilon^2\xi_X^{(2)}(\boldsymbol{r}) + \cdots. \qquad (55) \end{aligned}$$

The linear contribution is then given by $\xi_X^{(1)} = \partial\xi_X/\partial\epsilon|_{\epsilon=0}$.

Using the identities

$$\frac{\partial}{\partial\epsilon}\det\mathbf{B} = (\det\mathbf{B})\,{\rm Tr}\left[\mathbf{B}^{-1}\frac{\partial\mathbf{B}}{\partial\epsilon}\right], \qquad (56)$$

$$\frac{\partial\mathbf{B}^{-1}}{\partial\epsilon} = -\mathbf{B}^{-1}\frac{\partial\mathbf{B}}{\partial\epsilon}\mathbf{B}^{-1}, \qquad (57)$$

we have

$$\begin{aligned} \frac{\partial\xi_X}{\partial\epsilon} &= \int \frac{d^3q}{(2\pi)^{3/2}|B|^{1/2}}\, e^{-\frac{1}{2}(\boldsymbol{r}-\boldsymbol{q})^\top\mathbf{B}^{-1}(\boldsymbol{r}-\boldsymbol{q})} \\ &\times \left[\frac{1}{2}(\boldsymbol{r}-\boldsymbol{q})^\top\mathbf{B}^{-1}\mathbf{A}\mathbf{B}^{-1}(\boldsymbol{r}-\boldsymbol{q}) - \frac{1}{2}{\rm Tr}(\mathbf{B}^{-1}\mathbf{A})\right. \\ &+ \left. 2\langle F'\rangle \boldsymbol{U}^\top\mathbf{B}^{-1}(\boldsymbol{r}-\boldsymbol{q}) + \langle F'\rangle^2\xi_L + O(\epsilon)\right] \qquad (58)\\ &\overset{\epsilon\to 0}{=} \int \frac{d^3q}{(2\pi)^{3/2}\beta^3}\, e^{-(\boldsymbol{r}-\boldsymbol{q})^2/2\beta^2}\left[\frac{1}{2}\beta^{-4}(\boldsymbol{r}-\boldsymbol{q})^\top\mathbf{A}(\boldsymbol{r}-\boldsymbol{q})\right. \\ &- \left.\frac{1}{2}\beta^{-2}\,{\rm Tr}\,\mathbf{A} + 2\langle F'\rangle\beta^{-2}\boldsymbol{U}^\top(\boldsymbol{r}-\boldsymbol{q}) + \langle F'\rangle^2\xi_L\right]. \qquad (59) \end{aligned}$$

Integrating by parts, and noting that

$$\lim_{\beta\to 0}\frac{1}{(2\pi)^{3/2}\beta^3}\, e^{-(\boldsymbol{r}-\boldsymbol{q})^2/2\beta^2} = \delta_D(\boldsymbol{r}-\boldsymbol{q}), \qquad (60)$$

we obtain

$$\xi_X^{(1)}(\boldsymbol{r}) = \frac{1}{2}\frac{\partial^2 A_{ij}}{\partial r_i\partial r_j}(\boldsymbol{r}) - 2\langle F'\rangle\frac{\partial U_i}{\partial r_i}(\boldsymbol{r}) + \langle F'\rangle^2\xi_L(\boldsymbol{r}). \qquad (61)$$

We see immediately from Eq. (52) that

$$\frac{\partial^2 A_{ij}}{\partial q_i\partial q_j}(\boldsymbol{q}) = 2\xi_L(\boldsymbol{q}), \quad \frac{\partial U_i}{\partial q_i}(\boldsymbol{q}) = -\xi_L(\boldsymbol{q}). \qquad (62)$$

Therefore the linear theory limit of our result is

$$\xi_X^{(1)}(\boldsymbol{r}) = [1 + \langle F' \rangle]^2\, \xi_L(\boldsymbol{r}), \tag{63}$$

in agreement with standard perturbation theory.

4 HIGHER ORDER

We now repeat the derivation of the previous section, this time with the aim of extending our result to one order beyond the Zel'dovich approximation. Many of the technical details are relegated to appendices.

We pick up the track following Eq. (21), prior to which we make no use of the Zel'dovich approximation. With the help of the multinomial theorem, the cumulant expansion of Eq. (21) in the general case can be written

$$\log K = \sum_{N=1}^{\infty} \frac{i^N}{N!} \left\langle (\lambda_1\delta_1 + \lambda_2\delta_2 + \boldsymbol{k}\cdot\boldsymbol{\Delta})^N \right\rangle_c \tag{64}$$

$$= \sum_{m,n,r} \frac{i^{m+n+r}}{m!n!r!} \lambda_1^m \lambda_2^n k_{i_1} \ldots k_{i_r} \left\langle \delta_1^m \delta_2^n \Delta_{i_1} \ldots \Delta_{i_r} \right\rangle_c . \tag{65}$$

The cumulants $\left\langle \delta_1^m \delta_2^n \Delta_{i_1} \ldots \Delta_{i_r} \right\rangle_c$ are the key ingredients in our theory. In the following we refer to them generally as "Lagrangian correlators." As emphasized previously, they are functions of $\boldsymbol{q}$ only, so their tensor structure places severe restrictions on their functional form (see Appendix B). Moreover, due to the properties of Gaussian random fields, a cumulant of order $m + n + r$ must be at least of order $m + n + r - 1$ in the linear power spectrum P_L (e.g. Bernardeau et al. 2002). An expansion in cumulant order therefore corresponds to a perturbative expansion in powers of P_L.

For convenience, we assign different symbols to these Lagrangian correlators based on their tensor rank r. For $r = 0$, since δ_R is Gaussian, the only non-vanishing cumulants are

$$\langle \delta_1^2 \rangle_c = \langle \delta_2^2 \rangle_c \equiv \sigma_R^2, \qquad \langle \delta_1 \delta_2 \rangle_c \equiv \xi_R(\boldsymbol{q}). \tag{66}$$

For $r = 1$, 2, and 3 we denote

$$U_i^{mn} \equiv \langle \delta_1^m \delta_2^n \Delta_i \rangle_c, \tag{67}$$

$$A_{ij}^{mn} \equiv \langle \delta_1^m \delta_2^n \Delta_i \Delta_j \rangle_c, \tag{68}$$

$$W_{ijk}^{mn} \equiv \langle \delta_1^m \delta_2^n \Delta_i \Delta_j \Delta_k \rangle_c \quad . \tag{69}$$

Explicit expressions for these quantities may be found in Appendix B. Since they arise frequently, and to remain consistent with the previous section, we also adopt the shorthand

$$U_i^{10} \to U_i, \quad A_{ij}^{00} \to A_{ij}, \quad \text{and } W_{ijk}^{00} \to W_{ijk}. \tag{70}$$

In this notation, we evaluate Eq. (65) up to cumulants of order three,

$$\begin{aligned} \log K \;=\;& -\frac{1}{2}(\lambda_1^2 + \lambda_2^2)\sigma_R^2 - \frac{1}{2}A_{ij}k_ik_j - \lambda_1\lambda_2\xi_R \\ &- (\lambda_1+\lambda_2)U_ik_i - \frac{i}{6}W_{ijk}k_ik_jk_k - \frac{i}{2}(\lambda_1+\lambda_2)A_{ij}^{10}k_ik_j \\ &- \frac{i}{2}(\lambda_1^2 + \lambda_2^2)U_i^{20}k_i - i\lambda_1\lambda_2U_i^{11}k_i + O(P_L^3). \end{aligned} \tag{71}$$

We recover K by exponentiating. Of the eight terms in the above expression, only the first two have non-zero limits as $|\boldsymbol{q}| \to \infty$, *and* include $O(P_L)$ contributions. As in the Zel'dovich case, we leave these two terms exponentiated while expanding the rest, thus

$$\begin{aligned} K \;=\;& e^{-\frac{1}{2}(\lambda_1^2+\lambda_2^2)\sigma_R^2 - \frac{1}{2}A_{ij}k_ik_j}\Big[1 - \lambda_1\lambda_2\xi_R - (\lambda_1+\lambda_2)U_ik_i + \frac{1}{2}\lambda_1^2\lambda_2^2\xi_R^2 \\ &+ \frac{1}{2}(\lambda_1+\lambda_2)^2U_iU_jk_ik_j + \lambda_1\lambda_2(\lambda_1+\lambda_2)\xi_RU_ik_i \\ &- \frac{i}{6}W_{ijk}k_ik_jk_k - \frac{i}{2}(\lambda_1+\lambda_2)A_{ij}^{10}k_ik_j - \frac{i}{2}(\lambda_1^2+\lambda_2^2)U_i^{20}k_i \\ &- i\lambda_1\lambda_2U_i^{11}k_i + O(P_L^3)\Big]. \end{aligned} \tag{72}$$

As in Section 3.2, we must now integrate with respect to λ_1, λ_2, $\boldsymbol{k}$, and $\boldsymbol{q}$. The analog of Eq. (41) for the one-loop case is

$$\begin{aligned} L \;=\;& e^{-\frac{1}{2}A_{ij}k_ik_j}\Big[1 + \langle F'\rangle^2\xi_R + 2i\langle F'\rangle U_ik_i + \frac{1}{2}\langle F''\rangle^2\xi_R^2 \\ &- (\langle F''\rangle + \langle F'\rangle^2)U_iU_jk_ik_j + 2i\langle F'\rangle\langle F''\rangle\xi_RU_ik_i \\ &- \frac{i}{6}W_{ijk}k_ik_jk_k - \langle F'\rangle A_{ij}^{10}k_ik_j + i\langle F''\rangle U_i^{20}k_i \\ &+ i\langle F'\rangle^2U_i^{11}k_i + O(P_L^3)\Big], \end{aligned} \tag{73}$$

Analogous to Eq. (44), the $\boldsymbol{k}$ integration gives (see Appendix C)

$$\begin{aligned} M \;=\;& \frac{1}{(2\pi)^{3/2}|A|^{1/2}}\, e^{-\frac{1}{2}(\boldsymbol{r}-\boldsymbol{q})^T\mathbf{A}^{-1}(\boldsymbol{r}-\boldsymbol{q})}\Big[1 + \langle F'\rangle^2\xi_R \\ &- 2\langle F'\rangle U_ig_i + \frac{1}{2}\langle F''\rangle^2\xi_R - [\langle F''\rangle + \langle F'\rangle^2]U_iU_jG_{ij} \\ &- 2\langle F'\rangle\langle F''\rangle\xi_RU_ig_i + \frac{1}{6}W_{ijk}\Gamma_{ijk} - \langle F'\rangle A_{ij}^{10}G_{ij} \\ &- \langle F''\rangle U_i^{20}g_i - \langle F'\rangle^2U_i^{11}g_i + O(P_L^3)\Big]. \end{aligned} \tag{74}$$

where g_i and G_{ij} are defined in Eq. (45), and

$$\Gamma_{ijk} \equiv (A^{-1})_{ij}g_k + (A^{-1})_{ki}g_j + (A^{-1})_{jk}g_i - g_ig_jg_k, \tag{75}$$

Our final expression for the real-space correlation function $\xi_X(\boldsymbol{r})$ is given once again by Eq. (46), with $M(\boldsymbol{r},\boldsymbol{q})$ given by Eq. (74) up to $O(P_L^2)$. The redshift-space correlation function $\xi_X^s(\boldsymbol{s})$ is obtained by replacing the real-space Lagrangian correlators by their redshift-space counterparts.

5 RESULTS

Having presented the formalism and rationale behind our resummation, we now compare the results of our "convolution Lagrangian Perturbation Theory" (CLPT) to linear theory and to the earlier work of Matsubara (2008a,b). This is the most natural comparison, since our work is largely an extension of LRT and a partial resummation of that formalism.

Fig. 1 shows the (monopole) matter correlation function in real- and redshift-space. The solid line shows linear theory while the dashed and dotted lines show our CLPT and Matsubara's LRT respectively. In redshift-space we have used the formalism of Kaiser (1987) as our "linear theory". The points are from the N-body simulations described in Reid & White (2011); White et al. (2011). Throughout this paper we compare exclusively with $z = 0.55$ simulation outputs. Note that linear theory provides a poor approximation near the peak of the correlation function (at $100\,h^{-1}$Mpc) in both real- and redshift-space, as is well known and we have discussed previously. On large scales LRT and CLPT are nearly indistinguishable, as expected. However on smaller scales

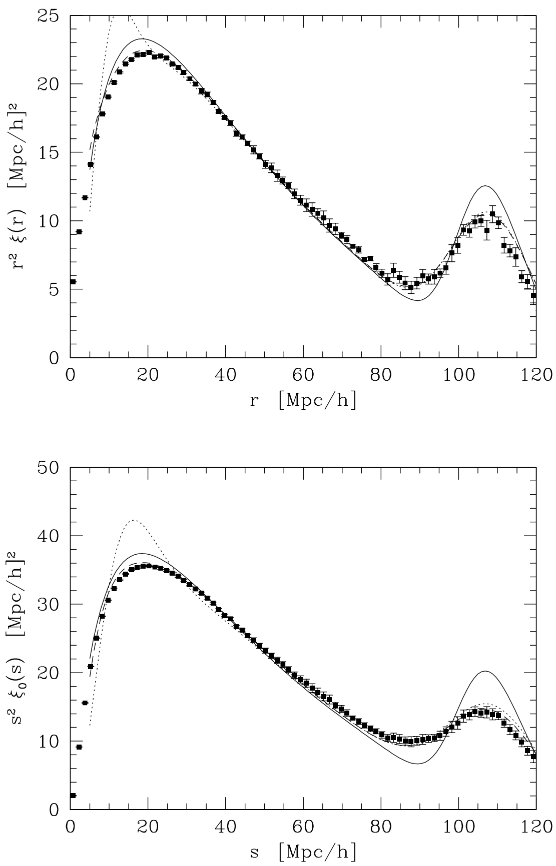

Figure 1. (Top) The real-space, matter correlation function, $\xi(r)$, from linear theory (solid), LRT (dotted) and CLPT (dashed) compared to N-body simulations (squares) at $z = 0.55$. In order to plot the results with a linear y-axis we have multiplied ξ by r^2, which removes much of the trend from $r \simeq 0 - 100$Mpc. LRT and CLPT agree very well on large scales (the lines can barely be distinguished) and agree well with the N-body results. LRT overshoots the N-body results below $r \simeq 20\,h^{-1}$Mpc while CLPT tracks the N-body results to much smaller scales. Linear theory overshoots at $r \simeq 20\,h^{-1}$Mpc and at $r \simeq 100\,h^{-1}$Mpc. (Bottom) The redshift-space, monopole, matter correlation function, $\xi_0(s)$, from linear theory (solid), LRT (dotted) and CLPT (dashed) compared to N-body simulations (squares). The qualitative behavior is as for $\xi(r)$.

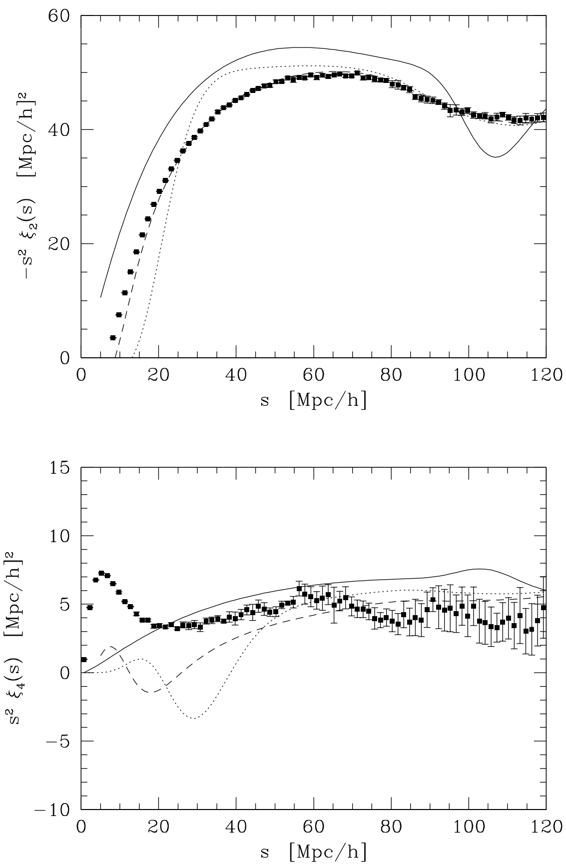

Figure 2. The redshift-space, quadrupole and hexadecapole, matter correlation functions, $\xi_2(s)$ and $\xi_4(s)$, from linear theory (solid), LRT (dotted) and CLPT (dashed) compared to N-body simulations (squares) at $z = 0.55$. For the quadrupole LRT and CLPT agree very well on large scales (and agree well with the N-body results) but LRT departs from the N-body results at much larger scales. For the hexadecapole the disagreement between N-body, CLPT, LRT and linear theory breaks down at larger scales than for the quadrupole.

the resummation inherent in our approach allows CLPT to track the N-body results to smaller scales than LRT.

The comparison with the quadrupole and hexadecapole moments of the redshift-space correlation function is very similar (Fig. 2). Both LRT and CLPT provide a better fit than linear theory to the quadrupole and hexadecapole moments at large scales, but all theories depart from the N-body results at larger scales than for the monopole. The level of agreement is worse for the hexadecapole, but that moment is also quite small.

Fig. 3 compares the theories for biased tracers, in this case for halos in the range $12.8 < \lg M_h < 13.1$ at $z \simeq 0.55$ though other results are qualitatively similar (see Fig. 4). The situation is similar to that for the matter: linear theory provides a poor approximation at large scales, missing the smearing of the acoustic peak due to the motion of material. LRT tends to overshoot the N-body results at small scales, while CLPT provides a good match down to $O(10\,h^{-1}$Mpc). Note that we considered two distinct sets of biasing parameters. In Figs. 3 and 5 we allowed the "renormalized" bias parameters $\langle F'\rangle$ and $\langle F''\rangle$ to be adjusted independently, while in Fig. 4, we related the two using the peak-background split, as in Matsubara (2008b,c).

Finally we compare the monopole and quadrupole moments of the redshift space correlation function of halos to the predictions of CLPT in Fig. 5. The prediction of the monopole moment is in relatively good agreement with the N-body measurements, though the level of agreement at $\sim\,20\,h^{-1}$Mpc is clearly not as good as it was with the matter. The prediction for the quadrupole is much worse than it was for the matter.

On large scales the prediction for the quadrupole is dominated by the same terms as the matter and the term scaling as $\langle F'\rangle$. The CLPT prediction does not have as much power on small scales as the N-body results, which have more small-scale power compared to the large-scale power than was the case for the matter. The shortfall in power is shared by the terms which survive when $\langle F'\rangle = 0$ and by the terms which scale as $\langle F'\rangle$. The failure of our model to match the quadrupole moment on small and intermediate scales may be due to our assumption of local Lagrangian bias. While this approximation has received some support from

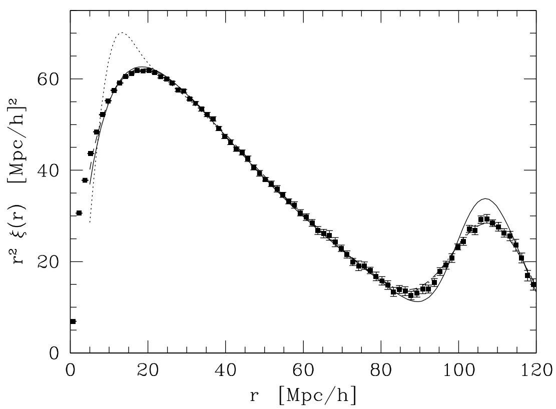

Figure 3. The real-space, correlation function for halos with $12.8 < \lg M_h < 13.1$ computed in linear theory (solid), LRT (dotted) and CLPT (dashed) compared to N-body simulations (squares) at $z = 0.55$. In this plot we allowed $\langle F' \rangle$ and $\langle F'' \rangle$ to vary independently to obtain the best agreement with the N-body results.

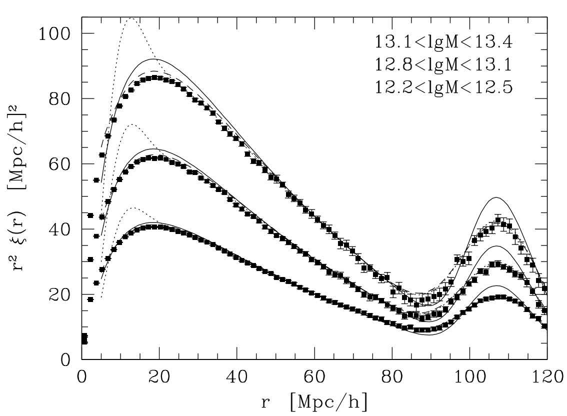

Figure 4. The real-space, correlation function for halos in three mass bins computed in linear theory (solid), LRT (dotted) and CLPT (dashed) compared to N-body simulations (squares) at $z = 0.55$ for three different mass ranges each a factor of two in width: from bottom to top $12.2 < \lg M_h < 12.5$, $12.8 < \lg M_h < 13.1$ and $13.1 < \lg M_h < 13.4$ with masses in $h^{-1} M_{\odot}$. In this plot we enforced the peak-background split relation to determine $\langle F'' \rangle$ in terms of the best fit $\langle F' \rangle$, i.e. the theory has only one free parameter.

N-body simulations (Roth & Porciani 2011; Baldauf et al. 2012; Chan, Scoccimarro, & Sheth 2012; Wang & Szalay 2012) we also expect that terms involving e.g. the tidal tensor, can become important for high mass halos (Sheth, Chan & Scoccimarro 2012). Such terms are naturally quadrupolar in nature and may affect the predictions.

6 DISCUSSION AND CONCLUSIONS

We have presented a new formulation of Lagrangian perturbation theory which allows accurate predictions of the low-multipole, real- and redshift-space correlation functions of the mass field and dark matter halos. Our formulation, which we refer to as "convolution Lagrangian perturbation theory" or CLPT involves a non-perturbative resummation and indeed can be viewed as a partial resummation of the formalism of Matsubara (2008a,b) upon which we have relied heavily.

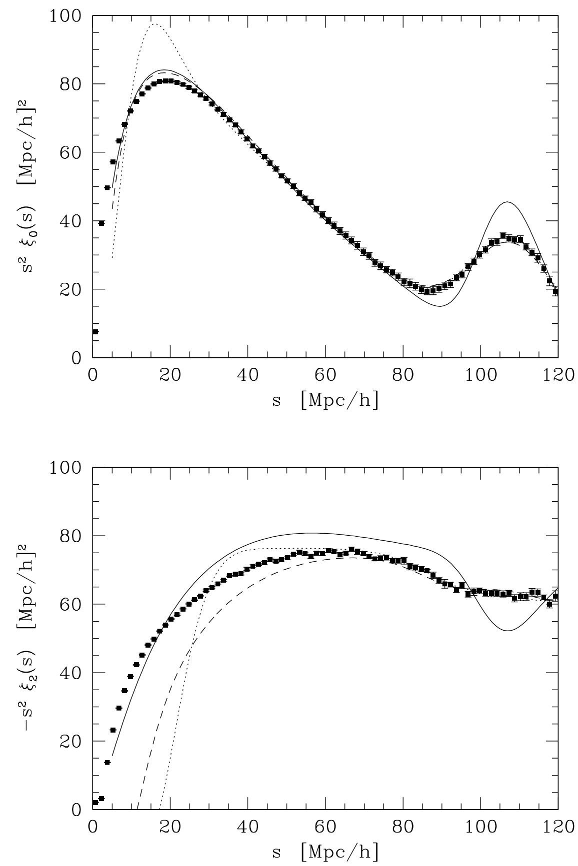

Figure 5. The redshift-space, monopole and quadrupole, correlation functions for halos computed in linear theory (solid), LRT (dotted) and CLPT (dashed) compared to N-body simulations (squares) at $z = 0.55$.

A key difference between CLPT and LRT or RPT is that we naturally recover the Zel'dovich approximation as the lowest order of our expansion for the matter correlation function. Tassev & Zaldarriaga (2012a) have recently emphasized the importance of not splitting the effects of bulk flows across orders in perturbation theory, and we find that CLPT (which does not make such a split) does indeed provide better agreement with N-body results at small scales than LRT (which does).

CLPT works best for the real-space clustering of the matter and halos and for the monopole of the redshift-space correlation functions. While the N-body results for the quadrupole and hexadecapole moments of the redshift-space correlation function for the matter is relatively well reproduced by CLPT, those moments for the halo correlation function differ significantly from the CLPT prediction. We suspect that this difference is due to a limitation in our bias prescription, in particular that our assumption of local Lagrangian bias for halos is not sufficiently accurate. Further work along these lines is clearly warranted.

One possible extension of this work is to use the real-space correlation function from CLPT in the Gaussian streaming model ansatz of Reid & White (2011) with v_{12} and σ_{12} terms calibrated from N-body simulations or computed within the context of LPT. These terms can be computed in our formalism by generalizing our function K (Eq. 21) to include a $\dot{\Delta}$ contribution and taking functional derivatives of K. We leave this for future work.

Finally, we note that our work may be relevant for efforts to model the bispectrum within the Lagrangian framework (e.g., Rampf & Wong 2012).

J.C. and M.W. are supported by the NSF and NASA. B.A.R. is supported by NASA. through Hubble Fellowship grant 51280 awarded by the Space Telescope Science Institute, which is operated by the Association of Universities for Research in Astronomy, Inc., for NASA, under contract NAS 5-26555. This work made extensive use of the NASA Astrophysics Data System and of the `astro-ph` preprint archive at `arXiv.org`. The analysis made use of the computing resources of the National Energy Research Scientific Computing Center.

REFERENCES

Baldauf T., Seljak U., Desjacques V., McDonald P., 2012, preprint [arXiv:1201.4827]
Bardeen J., Bond J., Kaiser N., Szalay A., 1986, ApJ, 304, 15
Bernardeau, F., Colombi, S., Gaztañaga, E., Scoccimarro, R., 2002, Physics Reports, 367, 1
Bharadwaj S., 1996, ApJ, 472, 1
Bond J.R., Couchman H.M.P., 1988, in the Proceedings of the Second Canadian Conference on General Relativity and Relativistic Astrophysics, p. 385
Buchert T., 1989, A&A, 223, 9
Carlson, J., White, M., Padmanabhan, N., 2009, PRD, 80, 043531
Catelan P., Lucchin F., Matarrese S., Porciani C., 1998, MNRAS, 297, 692
Chan K.C., Scoccimarro R., Sheth R., 2012, PRD, 85, 083509
Cole S., Fisher K.B., Weinberg D.H., 1994, MNRAS, 267, 785
Cooray, A., & Sheth, R. 2002, Physics Reports, 372, 1
Crocce M., Scoccimarro R., 2006, Phys. Rev. D73, 063519
Crocce M., Scoccimarro R., Bernardeau F., 2012, preprint [arXiv:1207.1465]
Efstathiou, G., Frenk, C., White, S., Davis, M., 1988, MNRAS, 235, 715
Eisenstein D., Seo H.-J., White M., 2007, ApJ, 664, 660
Elia A., Kulkarni S., Porciani C., Pietroni M., Matarrese S., 2011, MNRAS, 416 , 1703
Fisher K.B., 1995, ApJ, 448, 494
Hivon E., Bouchet F.R., Colombi S., Juszkiewicz R., 1995, A&A, 298, 643
Jennings, E., Baugh, C. M., Pascoli, S., 2011, MNRAS, 410, 2081
Jennings, E., Baugh, C. M., Pascoli, S., 2011, ApJL, 727, L9
Kaiser N., 1987, MNRAS, 227, 1
Matsubara T., 2008, Phys Rev D77, 063530
Matsubara T., 2008, Phys Rev D78, 083519
Matsubara T., 2008, Phys Rev D78, 109901
Matsubara, T., 2011, Phys Rev D83, 083518
McCullagh N., Szalay A., 2012, ApJ, 752, 21
Moutarde F., Alimi J.-M., Bouchet F.R., Pellat R., Ramani A., 1991, ApJ, 382, 377
Noh Y., White M., Padmanabhan N., 2009, Phys. Rev. D80, 123501
Okamura T., Taruya A., Matsubara T., 2011, JCAP, 8 ,12
Padmanabhan N., White M., Phys. Rev. D80, 063508
Padmanabhan N., White M., Cohn J.D., 2009, Phys. Rev. D79, 063523
Papai P., Szapudi I., 2008, MNRAS, 389, 292
Peacock J.A., 1992, MNRAS, 258, 581
Peebles P.J.E., 1976, Ap&SS, 45, 3
Peebles P.J.E., 1980, "The large-scale structure of the Universe", Princeton University Press (Princeton, 1980).
Rampf C., Buchert T., JCAP, 2012, 6, 21
Rampf C., 2012, preprint [arXiv:1205.5274]
Rampf C., Wong Y., JCAP, 2012, 6, 18
Reid B.A., White M., 2011, MNRAS, 417, 1913
Roth N., Porciani C., 2011, MNRAS, 415, 829
Samushia L., Pericval W., Raccanelli A., 2012, MNRAS, 420, 2102
Sato, M., Matsubara, T., 2011, Phys. Rev. D84, 04351
Scoccimarro R., 2004, Phys. Rev. D70, 083007
Seljak U., McDonald P., 2011, JCAP, 11, 39
Shaw J.R., Lewis A., 2008, Phys. Rev. D78, 103512
Sheth R., Chan K.C., Scoccimarro R., 2012, preprint [arXiv:1207.7117]
Taruya A., Nishimichi T., Saito S., 2010, Phys. Rev. D82, 063522
Taruya A., Saito S., Nishimichi T., 2011, Phys. Rev. D83, 103527 [arXiv:1101.4723]
Tassev S., Zaldarriaga M., 2012, JCAP, 4, 13
Tassev S., Zaldarriaga M., 2012, preprint [arXiv:1203.5785]
Taylor A.N., Hamilton A.J.S., 1996, MNRAS, 282, 767
Wang X., Szalay A., 2012, PRD, 86, 043508
White M., 2002, ApJS, 579, 16
White, M., Blanton, M., Bolton, A., et al. 2011, ApJ, 728, 126
Vlah Z., Seljak U., McDonald P., Okumura T., Baldauf T., 2012, preprint [arXiv:1207.0839]
Zel'dovich, Y., 1970, A&A, 5, 84

APPENDIX A: BIAS

As in Matsubara (2008b), we note the identity

$$\int \frac{d\lambda}{2\pi}\, \tilde{F}(\lambda) e^{-\frac{1}{2}\lambda^2\sigma_R^2} (i\lambda)^n = \left\langle F^{(n)} \right\rangle, \tag{A1}$$

where $\left\langle F^{(n)} \right\rangle$ is the expectation value of the nth derivative of the Lagrangian bias function, what are referred to as "renormalized" bias coefficients c_n in Matsubara 2011. The mapping $K \to L$ is therefore achieved by replacing

$$(\lambda_1 + \lambda_2) \to -2i \langle F' \rangle, \tag{A2}$$

$$\lambda_1 \lambda_2 \to -\langle F' \rangle^2, \tag{A3}$$

$$\lambda_1^2 \lambda_2^2 \to \langle F'' \rangle^2, \tag{A4}$$

$$(\lambda_1 + \lambda_2)^2 \to -2\left[\langle F'' \rangle + \langle F' \rangle^2\right], \tag{A5}$$

$$\lambda_1 \lambda_2 (\lambda_1 + \lambda_2) \to 2i \langle F' \rangle \langle F'' \rangle, \tag{A6}$$

$$\lambda_1^2 + \lambda_2^2 \to -2 \langle F'' \rangle. \tag{A7}$$

APPENDIX B: LAGRANGIAN CORRELATORS

In this appendix we collect the relevant facts and formulas concerning Lagrangian correlators that we need for our one-loop theory. The correlators are defined by

$$C^{mn}_{i_1\cdots i_r}(\boldsymbol{q}) = \left\langle \delta_1^m \delta_2^n \Delta_{i_1} \cdots \Delta_{i_r} \right\rangle_c, \tag{B1}$$

where $\delta_1 = \delta_L(\boldsymbol{q}_1)$, $\delta_2 = \delta_L(\boldsymbol{q}_2)$, and $\Delta_i = \Psi_i(\boldsymbol{q}_2) - \Psi_i(\boldsymbol{q}_1)$. The subscripted c refers to a connected moment; since these fields have zero mean, the connected moments coincide with normal expectation values for orders $m + n + r \leqslant 3$.

B1 Index structure

By translational symmetry, a Lagrangian correlator can only depend on the Lagrangian separation $\boldsymbol{q} = \boldsymbol{q}_2 - \boldsymbol{q}_1$. This imposes strong constraints on its index structure. We classify a correlator by its tensor rank, i.e. by the number of vector indices it carries. In the following we let U_i, A_{ij}, and W_{ijk} denote generic correlators of ranks 1, 2, and 3, respectively.

Rank-1 correlators must be of the form

$$U_i(\boldsymbol{q}) = U(q)\,\hat{q}_i \tag{B2}$$

for some scalar function $U(q)$, since (trivially) the only vector quantity that can be formed from the vector $\boldsymbol{q}$ is proportional to $\boldsymbol{q}$. Rank-2 correlators must involve only rotationally invariant rank-2 tensors that can be formed from the vector $\boldsymbol{q}$, i.e. δ_{ij} or $\hat{q}_i\hat{q}_j$. Thus their general form is

$$A_{ij}(\boldsymbol{q}) = X(q)\,\delta_{ij} + Y(q)\,\hat{q}_i\hat{q}_j. \tag{B3}$$

Likewise, rank-3 correlators are of the form

$$W_{ijk}(\boldsymbol{q}) = V_1(q)\,\hat{q}_i\delta_{jk} + V_2(q)\,\hat{q}_j\delta_{ki} + V_3(q)\,\hat{q}_k\delta_{ij} + T(q)\,\hat{q}_i\hat{q}_j\hat{q}_k. \tag{B4}$$

We remind the reader that we adopt the shorthand

$$U_i^{10} \to U_i, \quad A_{ij}^{00} \to A_{ij}, \quad \text{and } W_{ijk}^{00} \to W_{ijk}, \tag{B5}$$

since these combinations arise frequently.

In general, correlators of even rank are even functions of $\boldsymbol{q}$, while those of odd rank are odd. This implies that the correlator $C^{mn}_{i_1\ldots i_r}$ is symmetric in the indices m and n, as the following chain of equalities shows:

$$\begin{aligned}
C^{mn}_{i_1\ldots i_r}(\boldsymbol{q}) &= \left\langle \delta_1^m\delta_2^n\Delta_{i_1}\cdots\Delta_{i_r}\right\rangle_c \\
&= \left\langle \delta_L(\boldsymbol{q}_1)^m\delta_L(\boldsymbol{q}_2)^n[\Psi_{i_1}(\boldsymbol{q}_2) - \Psi_{i_1}(\boldsymbol{q}_1)]\cdots \right. \\
&\quad \left.\cdots[\Psi_{i_r}(\boldsymbol{q}_2) - \Psi_{i_r}(\boldsymbol{q}_1)]\right\rangle_c \\
&= (-1)^r \left\langle \delta_L(\boldsymbol{q}_2)^n\delta_L(\boldsymbol{q}_1)^m[\Psi_{i_1}(\boldsymbol{q}_1) - \Psi_{i_1}(\boldsymbol{q}_2)]\cdots \right. \\
&\quad \left.\cdots[\Psi_{i_r}(\boldsymbol{q}_1) - \Psi_{i_r}(\boldsymbol{q}_2)]\right\rangle_c \\
&= (-1)^r C^{nm}_{i_1\ldots i_r}(-\boldsymbol{q}) \\
&= C^{nm}_{i_1\ldots i_r}(\boldsymbol{q}).
\end{aligned} \tag{B6}$$

We can solve for the coefficients in these expansions by contracting against tensors and solving the resulting simultaneous equations, e.g. for the components of W_{ijk}:

$$\begin{aligned}
3V_1 + V_2 + V_3 + T &= W_{ijk}\,\hat{q}_i\delta_{jk}, \\
V_1 + 3V_2 + V_3 + T &= W_{ijk}\,\hat{q}_j\delta_{ki}, \\
V_1 + V_2 + 3V_3 + T &= W_{ijk}\,\hat{q}_k\delta_{ij}, \\
V_1 + V_2 + V_3 + T &= W_{ijk}\,\hat{q}_i\hat{q}_j\hat{q}_k.
\end{aligned} \tag{B7}$$

B2 Perturbative orders

The LPT expansion of the field $\boldsymbol{\Delta}$ has the form

$$\boldsymbol{\Delta} = \boldsymbol{\Delta}^{(1)} + \boldsymbol{\Delta}^{(2)} + \boldsymbol{\Delta}^{(3)} + \cdots, \tag{B8}$$

where $\boldsymbol{\Delta}^{(a)}$ involves a factors of the linear density field δ_L. The correlators $C^{mn}_{i_1\cdots i_r}$ may therefore be expanded as

$$C^{mn}_{i_1\cdots i_r} = \sum_{a_1=1}^{\infty}\cdots\sum_{a_r=1}^{\infty} C^{mn(a_1\cdots a_r)}_{i_1\cdots i_r}, \tag{B9}$$

where $C^{mn(a_1\cdots a_r)}_{i_1\cdots i_r} = \left\langle \delta_1^m\delta_2^n\Delta^{(a_1)}_{i_1}\cdots\Delta^{(a_r)}_{i_r}\right\rangle_c$. Since δ_L is Gaussian, many of these terms vanish. Here we display the breakdown for each of the quantities introduced in Section 4, up to order $O(P_L^2)$:

$$U_i = U_i^{(1)} + U_i^{(3)} + \cdots, \tag{B10}$$

$$A_{ij} = A_{ij}^{(11)} + A_{ij}^{(22)} + A_{ij}^{(13)} + A_{ij}^{(31)} + \cdots, \tag{B11}$$

$$W_{ijk} = W_{ijk}^{(112)} + W_{ijk}^{(121)} + W_{ijk}^{(211)} + \cdots, \tag{B12}$$

$$U_i^{20} = U_i^{20(2)} + \cdots, \tag{B13}$$

$$U_i^{11} = U_i^{11(2)} + \cdots, \tag{B14}$$

$$A_{ij}^{10} = A_{ij}^{10(12)} + A_{ij}^{10(21)} + \cdots, \tag{B15}$$

B3 Scalar components

Given the index structure described in the previous subsection, evaluating the Lagrangian correlators reduces to computing a set of scalar functions of q. In order to maintain notational consistency with Matsubara (2008b) we make use of his definitions of Q and R.

$$R_n(k) = \frac{k^3}{4\pi^2}P_L(k)\int_0^\infty dr\, P_L(kr)\widetilde{R}_n(r) \tag{B16}$$

and

$$Q_n(k) = \frac{k^3}{4\pi^2}\int_0^\infty dr\, P_L(kr)\int_{-1}^{1} dx\, P_L(k\sqrt{y})Q_n(r,x)\,, \tag{B17}$$

where $y(r,x) = 1 + r^2 - 2rx$ and the Q_n are given by

$$\begin{aligned}
Q_1 &= \frac{r^2(1-x^2)^2}{y^2}, \quad Q_2 = \frac{(1-x^2)rx(1-rx)}{y^2}, \\
Q_3 &= \frac{x^2(1-rx)^2}{y^2}, \quad Q_4 = \frac{1-x^2}{y^2}, \\
Q_5 &= \frac{rx(1-x^2)}{y}, \quad Q_6 = \frac{(1-3rx)(1-x^2)}{y}, \\
Q_7 &= \frac{x^2(1-rx)}{y}, \quad Q_8 = \frac{r^2(1-x^2)}{y}, \\
Q_9 &= \frac{rx(1-rx)}{y}, \quad Q_{10} = 1-x^2, \\
Q_{11} &= x^2,\ Q_{12} = rx,\ Q_{13} = r^2
\end{aligned}$$

and

$$\widetilde{R}_1(r) = \int_{-1}^{+1} dx\, \frac{r^2(1-x^2)^2}{1+r^2-2rx}$$

$$\widetilde{R}_2(r) = \int_{-1}^{+1} dx\, \frac{(1-x^2)rx(1-rx)}{1+r^2-2rx}$$

In the following, equation references prefaced with "M" indicate equations in Matsubara (2008b).

The expression for $A_{ij} = A_{ij}^{00}$ is derived in detail below. The other components we need are

$$A_{ij}^{10}(\boldsymbol{q}) = \langle\delta_1\Delta_i\Delta_j\rangle_c \tag{B18}$$

$$= X_{10}(q)\delta_{ij} + Y_{10}(q)\hat{q}_i\hat{q}_j \tag{B19}$$

with

$$\xi_L(q) = \frac{1}{2\pi^2}\int_0^\infty dk\, k^2 P_L(k) j_0(kq) \quad \text{(B20)}$$

$$V_1^{(112)}(q) = \frac{1}{2\pi^2}\int_0^\infty \frac{dk}{k}\left(-\frac{3}{7}\right) R_1 j_1(kq) \quad \text{(B21)}$$

$$V_3^{(112)}(q) = \frac{1}{2\pi^2}\int_0^\infty \frac{dk}{k}\left(-\frac{3}{7}\right) Q_1 j_1(kq) \quad \text{(B22)}$$

$$S^{(112)}(q) = \frac{1}{2\pi^2}\int_0^\infty \frac{dk}{k}\,\frac{3}{7}\left[2R_1 + 4R_2 + Q_1 + 2Q_2\right]\frac{j_2(kq)}{kq} \quad \text{(B23)}$$

$$T^{(112)}(q) = \frac{1}{2\pi^2}\int_0^\infty \frac{dk}{k}\left(-\frac{3}{7}\right)\times \left[2R_1 + 4R_2 + Q_1 + 2Q_2\right] j_3(kq) \quad \text{(B24)}$$

$$U^{(1)}(q) = \frac{1}{2\pi^2}\int_0^\infty dk\, k\,(-1) P_L(k) j_1(kq) \quad \text{(B25)}$$

$$U^{(3)}(q) = \frac{1}{2\pi^2}\int_0^\infty dk\, k\left(-\frac{5}{21}\right) R_1 j_1(kq) \quad \text{(B26)}$$

$$U_{20}^{(2)}(q) = \frac{1}{2\pi^2}\int_0^\infty dk\, k\left(-\frac{3}{7}\right) Q_8 j_1(kq) \quad \text{(B27)}$$

$$U_{11}^{(2)}(q) = \frac{1}{2\pi^2}\int_0^\infty dk\, k\left(-\frac{6}{7}\right)\left[R_1 + R_2\right] j_1(kq) \quad \text{(B28)}$$

$$X_{10}^{(12)}(q) = \frac{1}{2\pi^2}\int_0^\infty dk\, \frac{1}{14}\left\{2\left[R_1 - R_2\right] + 3R_1 j_0(kq) - 3\left[3R_1 + 4R_2 + 2Q_5\right]\frac{j_1(kq)}{kq}\right\} \quad \text{(B29)}$$

$$Y_{10}^{(12)}(q) = \frac{1}{2\pi^2}\int_0^\infty dk\left(-\frac{3}{14}\right)\left[3R_1 + 4R_2 + 2Q_5\right]\times \left[j_0(kq) - 3\frac{j_1(kq)}{kq}\right] \quad \text{(B30)}$$

where the arguments of the R_n and Q_n terms are k and have been omitted for brevity. The remaining equations, for $X^{(11)}$, $X^{(22)}$, $X^{(13)}$, $Y^{(11)}$, $Y^{(22)}$, $Y^{(13)}$ are presented and derived in the next section,

B4 Example

We provide here an example of how to obtain the formulae of the previous subsection. We focus on $A_{ij} = \langle \Delta_i \Delta_j \rangle_c$, since this is the most important of the Lagrangian correlators in our theory.

By the definition of $\boldsymbol{\Delta}$,

$$\Delta_i = \Psi_i(\boldsymbol{q}_2) - \Psi_i(\boldsymbol{q}_1) = \int \frac{d^3p}{(2\pi)^3}\left(e^{i\boldsymbol{p}\cdot\boldsymbol{q}_2} - e^{i\boldsymbol{p}\cdot\boldsymbol{q}_1}\right)\tilde{\Psi}_i(\boldsymbol{p}), \quad \text{(B31)}$$

and therefore

$$A_{ij} = \int \frac{d^3p_1}{(2\pi)^3}\frac{d^3p_2}{(2\pi)^3}\left(e^{i\boldsymbol{p}_1\cdot\boldsymbol{q}_2} - e^{i\boldsymbol{p}_1\cdot\boldsymbol{q}_1}\right)\left(e^{i\boldsymbol{p}_2\cdot\boldsymbol{q}_2} - e^{i\boldsymbol{p}_2\cdot\boldsymbol{q}_1}\right) \times \left\langle \tilde{\Psi}_i(\boldsymbol{p}_1)\tilde{\Psi}_j(\boldsymbol{p}_2)\right\rangle_c . \quad \text{(B32)}$$

From Eq. (M.A9), the Fourier space 2-point function here is

$$\left\langle \tilde{\Psi}_i(\boldsymbol{p}_1)\tilde{\Psi}_j(\boldsymbol{p}_2)\right\rangle_c = -(2\pi)^3\delta_D^3(\boldsymbol{p}_1 + \boldsymbol{p}_2) C_{ij}(\boldsymbol{p}_1). \quad \text{(B33)}$$

The quantity $C_{ij}(\boldsymbol{k})$ here has contributions at both tree and 1-loop level,

$$C_{ij}^{(11)}(\boldsymbol{k}) = -\frac{k_i k_j}{k^4} P_L(k), \quad \text{(M.A52)}$$

$$C_{ij}^{(22)}(\boldsymbol{k}) = -\frac{9}{98}\frac{k_i k_j}{k^4} Q_1(k), \quad \text{(M.A53)}$$

$$C_{ij}^{(13)}(\boldsymbol{k}) = C_{ij}^{(31)}(\boldsymbol{k}) = -\frac{5}{21}\frac{k_i k_j}{k^4} R_1(k). \quad \text{(M.A54)}$$

These terms are all of the form $C_{ij} = -(k_i k_j/k^4) a(k)$ for scalar $a(k)$, as is guaranteed by rotational symmetry. With the substitution of Eq. (B33) into Eq. (B32), we have

$$A_{ij} = \int \frac{d^3k}{(2\pi)^3}\left(2 - e^{i\boldsymbol{k}\cdot\boldsymbol{q}} - e^{-i\boldsymbol{k}\cdot\boldsymbol{q}}\right)\frac{k_i k_j}{k^4} a(k). \quad \text{(B34)}$$

Contracting this quantity first by δ_{ij} and then by $\hat{q}_i\hat{q}_j$, we obtain the system of equations

$$A_{ij}\delta_{ij} = 3X + Y = \int \frac{d^3k}{(2\pi)^3}\left(2 - e^{i\boldsymbol{k}\cdot\boldsymbol{q}} - e^{-i\boldsymbol{k}\cdot\boldsymbol{q}}\right)\frac{1}{k^2} a(k), \quad \text{(B35)}$$

$$A_{ij}\hat{q}_i\hat{q}_j = X + Y = \int \frac{d^3k}{(2\pi)^3}\left(2 - e^{i\boldsymbol{k}\cdot\boldsymbol{q}} - e^{-i\boldsymbol{k}\cdot\boldsymbol{q}}\right)\frac{(\hat{k}\cdot\hat{q})^2}{k^2} a(k). \quad \text{(B36)}$$

Letting $\mu = \hat{k}\cdot\hat{q}$ and using the Bessel function identities in Appendix C we may perform the angular integrations,

$$3X + Y = \frac{1}{2\pi^2}\int_0^\infty k^2 dk \frac{1}{2}\int_{-1}^1 d\mu\left(2 - e^{ikq\mu} - e^{-ikq\mu}\right)\frac{1}{k^2} a(k) = \frac{1}{2\pi^2}\int_0^\infty dk\left[2 - 2j_0(kq)\right] a(k), \quad \text{(B37)}$$

$$X + Y = \frac{1}{2\pi^2}\int_0^\infty k^2 dk \frac{1}{2}\int_{-1}^1 d\mu\left(2 - e^{ikq\mu} - e^{-ikq\mu}\right)\frac{\mu^2}{k^2} a(k) = \frac{1}{2\pi^2}\int_0^\infty dk\left[\frac{2}{3} - 2j_0(kq) + 4\frac{j_1(kq)}{kq}\right] a(k), \quad \text{(B38)}$$

from which we obtain

$$X(q) = \frac{1}{2\pi^2}\int_0^\infty dk\, a(k)\left[\frac{2}{3} - 2\frac{j_1(kq)}{kq}\right], \quad \text{(B39)}$$

$$Y(q) = \frac{1}{2\pi^2}\int_0^\infty dk\, a(k)\left[-2j_0(kq) + 6\frac{j_1(kq)}{kq}\right]. \quad \text{(B40)}$$

Explicitly, up to 1-loop order, the contributions to $X(q)$ and $Y(q)$ are

$$X^{(11)}(q) = \frac{1}{2\pi^2}\int_0^\infty dk\, P_L(k)\left[\frac{2}{3} - 2\frac{j_1(kq)}{kq}\right], \quad \text{(B41)}$$

$$X^{(22)}(q) = \frac{1}{2\pi^2}\int_0^\infty dk\, \frac{9}{98} Q_1(k)\left[\frac{2}{3} - 2\frac{j_1(kq)}{kq}\right], \quad \text{(B42)}$$

$$X^{(13)}(q) = \frac{1}{2\pi^2}\int_0^\infty dk\, \frac{5}{21} R_1(k)\left[\frac{2}{3} - 2\frac{j_1(kq)}{kq}\right], \quad \text{(B43)}$$

$$Y^{(11)}(q) = \frac{1}{2\pi^2}\int_0^\infty dk\, P_L(k)\left[-2j_0(kq) + 6\frac{j_1(kq)}{kq}\right], \quad \text{(B44)}$$

$$Y^{(22)}(q) = \frac{1}{2\pi^2}\int_0^\infty dk\, \frac{9}{98} Q_1(k)\left[-2j_0(kq) + 6\frac{j_1(kq)}{kq}\right], \quad \text{(B45)}$$

$$Y^{(13)}(q) = \frac{1}{2\pi^2}\int_0^\infty dk\, \frac{5}{21} R_1(k)\left[-2j_0(kq) + 6\frac{j_1(kq)}{kq}\right]. \quad \text{(B46)}$$

Note that each of these quantities approaches 0 as $q \to 0$.

APPENDIX C: REFERENCE FORMULAE

C1 Gaussian integrals

In our theory we make use of the basic Gaussian integral

$$Q(\boldsymbol{b}) \equiv \int \frac{d^3k}{(2\pi)^3} e^{-\frac{1}{2}\boldsymbol{k}^T \mathbf{A}\boldsymbol{k} + i\boldsymbol{b}\cdot\boldsymbol{k}} = \frac{1}{(2\pi)^{3/2}|A|^{1/2}} e^{-\frac{1}{2}\boldsymbol{b}^T\mathbf{A}^{-1}\boldsymbol{b}}. \quad \text{(C1)}$$

where $|A|$ denotes the determinant of the 3×3 matrix $\mathbf{A}$. By successive applications of the operator $-i\partial/\partial b_i$, we also have

$$\int \frac{d^3k}{(2\pi)^3}\, G(\mathbf{k})k_i = i(\mathbf{A}^{-1}\boldsymbol{b})_i Q(\boldsymbol{b}) \quad , \tag{C2}$$

$$\int \frac{d^3k}{(2\pi)^3}\, G(\mathbf{k})k_i k_j = \left[(\mathbf{A}^{-1})_{ij} - (\mathbf{A}^{-1}\boldsymbol{b})_i(\mathbf{A}^{-1}\boldsymbol{b})_j\right] Q(\boldsymbol{b}), \tag{C3}$$

$$\begin{aligned}\int \frac{d^3k}{(2\pi)^3}\, G(\mathbf{k})k_i k_j k_k &= i\Big[(\mathbf{A}^{-1})_{ij}(\mathbf{A}^{-1}\boldsymbol{b})_k + (\mathbf{A}^{-1})_{ki}(\mathbf{A}^{-1}\boldsymbol{b})_j \\ &+ (\mathbf{A}^{-1})_{jk}(\mathbf{A}^{-1}\boldsymbol{b})_i \\ &- (\mathbf{A}^{-1}\boldsymbol{b})_i(\mathbf{A}^{-1}\boldsymbol{b})_j(\mathbf{A}^{-1}\boldsymbol{b})_k\Big] Q(\boldsymbol{b}).\end{aligned} \tag{C4}$$

where we have written

$$G(\mathbf{k}) = e^{-\frac{1}{2}\boldsymbol{k}^T\mathbf{A}\boldsymbol{k} + i\boldsymbol{b}\cdot\boldsymbol{k}} \tag{C5}$$

for notational compactness.

C2 Spherical Bessel functions

In performing the integrals in the previous sections we have found the following spherical Bessel function identities and integrals to be useful:

$$j_{n-1}(x) + j_{n+1}(x) = (2n+1)\frac{j_n(x)}{x} \tag{C6}$$

$$n\,j_{n-1}(x) - (n+1)\,j_{n+1}(x) = (2n+1)\frac{d}{dx}j_n(x) \tag{C7}$$

$$\frac{1}{2}\int_{-1}^{1} d\mu\, e^{ix\mu} = j_0(x) \tag{C8}$$

$$\frac{1}{2}\int_{-1}^{1} d\mu\, \mu\, e^{ix\mu} = i\,j_1(x) \tag{C9}$$

$$\frac{1}{2}\int_{-1}^{1} d\mu\, \mu^2\, e^{ix\mu} = \frac{1}{3}j_0(x) - \frac{2}{3}j_2(x) \tag{C10}$$

$$= j_0(x) - 2\frac{j_1(x)}{x} \tag{C11}$$

$$\frac{1}{2}\int_{-1}^{1} d\mu\, \mu^3\, e^{ix\mu} = i\left[\frac{3}{5}j_1(x) - \frac{2}{5}j_3(x)\right] \tag{C12}$$